DOI: 10.21062/mft.2026.021 http://www.journalmt.com

Finite Element Secondary Development of Constitutive Model for Titanium Alloy Vibration-Assisted Cold Upsetting Forming

Xu Yani (0009-0009-7387-0713), Wang Ying (0000-0001-5687-1049)*, Wei Chuhan (0009-0004-2397-7452), Lin Kai (0009-0009-6095-2218), Shu Xuedao (0000-0001-9928-7344)
School of Mechanical Engineering and Intelligent Manufacturing, Ningbo University, No. 818 Fenghua Road, Jiangbei District, Ningbo, Zhejiang Province, China. E-mail: wangying5@nbu.edu.cn.

To achieve precise finite element simulation of the vibration-assisted cold upsetting forming process of titanium alloys, this study focuses on Ti-45Nb titanium alloy as the research object. A constitutive model for vibration-assisted cold upsetting forming is established, incorporating both viscoelastic and viscoplastic deformation. The model is transformed into a programmable incremental form, and the control equations for elastic-viscoplastic deformation are derived. Secondary development is conducted using the VUMAT interface of ABAQUS, and the model is applied in simulation. Multi-condition simulations of Ti-45Nb titanium alloy cold upsetting forming are performed, and the results are compared with experimental data. The average relative error is found to be within 5%, verifying the accuracy of the finite element numerical simulation based on the secondary development. The developed constitutive model is used to simulate the cold upsetting forming process of Ti-45Nb titanium alloy internal wire joint components. The significant effects of vibration assistance in reducing maximum stress, optimizing stress distribution, and improving material flow are intuitively observed. This study provides technical support for the application of vibration-assisted cold upsetting forming technology in the forming of difficult-to-deform materials.

Keywords: Cold upsetting forming, Vibration assistance, VUMAT subroutine, Constitutive model, Finite element simulation

1 Introduction

Multi-station cold upsetting is a non-cutting metal pressure working process with low consumption, high material yield, and high production efficiency [1,2]. With the development of high-end manufacturing industries such as aeronautics, astronautics, and high-speed trains in China, the demand for high-strength fasteners, represented by titanium alloys, is increasing [3-5]. However, at room temperature, titanium alloys have high deformation resistance and severe work hardening, which makes them difficult to form and limits the application of cold upsetting processes.

Vibration-assisted plastic forming technology, applied in the forming process in the form of mechanical vibration or ultrasonic vibration, can effectively alter the internal stress distribution and flow characteristics of materials, making them more susceptible to flow and cavity filling during forming [6]. Applying auxiliary vibration during forming is an effective method for achieving high-speed cold upsetting forming of titanium alloy fasteners at room temperature [7-9]. However, due to the short duration of vibration-assisted cold upsetting forming, it is challenging to monitor stress-strain distribution and workpiece geometric changes during the process [10]. Finite element simulation technology is therefore utilized to reveal complex phenomena such as material flow, stress distribution, and temperature changes during forming, serving as a primary research method for vibration-assisted cold upsetting forming.

The accuracy of numerical simulation results depends on the precision of the material constitutive equation [11-12]. Research on constitutive theory for vibration-assisted forming shows that Kirchner et al. [13] established a compression stress oscillation superposition model for materials with strain rate - independent and - dependent plasticity, highlighting significant stress differences between the two under low-frequency vibration. Cai et al. [14] proposed a vibration-assisted tension constitutive model, demonstrating the strong predictive capability of viscoelastic-viscoplastic models for metal mechanical properties under vibration. Wang [15] developed a constitutive model for 6061 aluminum alloy based on Cai's model, validating its reliability in ultrasonic vibration-assisted tensile tests. Siddiq et al. [16-17] incorporated acoustic softening effects into crystal models for vibration-assisted forming, improving the accuracy of phenomenological constitutive models. These findings indicate that constitutive models under vibration-assisted conditions are becoming more sophisticated. However, the integration of these theoretical achievements into practical applications

through secondary development of finite element software remains a gap. Such development is vital for advancing vibration-assisted cold upsetting forming technology, as it enables seamless integration of complex constitutive models, improves simulation accuracy, customizes calculation processes, enhances simulation efficiency, and optimizes process parameters to improve material utilization and product yield [18].

This study focuses on Ti-45Nb titanium alloy to establish a constitutive model for vibration-assisted cold upsetting forming that considers viscoelasticity and viscoplasticity. The model is integrated into finite element simulations through secondary development of the software, providing a theoretical basis for investigating the dynamic mechanical properties of Ti-45Nb titanium alloy under vibration-assisted cold upsetting forming.

2 Constitutive Model Development

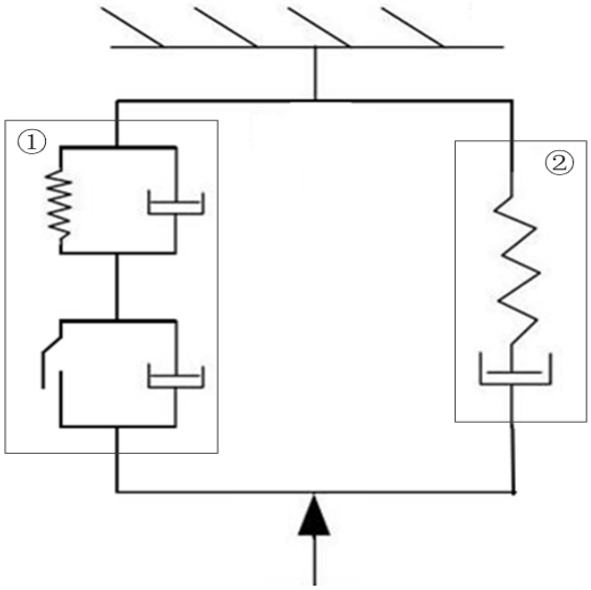

Fig. 1 *Visco-elastoplastic Model*

Based on plasticity theory for large deformation and existing visco-elastoplastic theories [19], a hybrid constitutive model considering stress superposition and softening effects was developed for multi-pass cold upsetting forming of Ti-45Nb titanium alloy under vibration assistance, as shown in Fig. 1.

In the first mechanism, the stress superposition effect caused by vibration is described by a series connection of elastic and viscoplastic components. Combining Voigt and Kelvin models, the viscoelastic-viscoplastic stress can be expressed as [20]:

$$\sigma^{(1)} = \frac{\eta_1}{\eta_1+\eta_2} E\varepsilon + \frac{\eta_1\eta_2}{\eta_1+\eta_2}\dot{\varepsilon} + \sigma_i \tag{1}$$

Where:

η_1 and η_2 …Material viscosity coefficients,

E …The elastic modulus,

ε …The material strain.

$\dot{\varepsilon}$ …The material strain rate.

The first term on the right denotes the elastic stress change under vibration. The second term represents the change in viscous stress under vibration, reflecting the stress superposition effect of vibration, that is, periodic fluctuations superimposed on the original stress and strain, The third term denotes the plastic stress component.

The second mechanism reflects the softening effect produced during metal deformation. As vibration energy increases, the stress reduction process can be expressed as [20]:

$$\sigma^{(2)} = 2\hat{\tau}\theta\left(E_u/\hat{\tau}\right)^n \tag{2}$$

Where:

θ and n …Vibration energy field parameters,

$\hat{\tau}$ …The material's shear threshold,

E_u …Denotes acoustic energy.

Combining Eqs. (1) and (2), the constitutive model can be expressed as:

$$\sigma = \sigma^{(1)} - \sigma^{(2)} = \frac{\eta_1}{\eta_1+\eta_2} E\varepsilon + \frac{\eta_1\eta_2}{\eta_1+\eta_2}\dot{\varepsilon} + \sigma_i - 2\hat{\tau}\theta\left(E_u/\hat{\tau}\right)^n \tag{3}$$

3 Constitutive Model Algorithm Derivation

In the initial deformation stage, material units undergo elastic deformation, $\Delta\varepsilon = \Delta\varepsilon^e$, resulting in elastic strain. Based on the initial stress tensor σ_{old} of the incremental step, the elastic predicted stress tensor can be obtained as:

$$\sigma^{tr} = \sigma_{old} + \lambda trace(\varepsilon)I + 2G\Delta\varepsilon \tag{4}$$

Where:

$trace(\varepsilon)$ …The trace of the tensor;

I …The unit tensor;

λ and G …The first Lame and constant the material's shear modulus, respectively, which can be expressed in terms of the elastic modulus E and Poisson's ratio ν as:

$$\lambda = \frac{v}{(1+v)(1-2v)} E \tag{5}$$

$$G = \frac{1}{2(1+v)} E \tag{6}$$

For stress in metal materials, it can generally be decomposed into spherical stress tensors σ_m (hydrostatic stress) and deviatoric stress tensors $\boldsymbol{S}$. The spherical stress tensor induces elastic deformation in materials, while the deviatoric stress tensor induces plastic deformation. The specific expressions are as follows:

$$\sigma_{\mathrm{m}} = \frac{1}{3}(\sigma_{11} + \sigma_{22} + \sigma_{33}) \tag{7}$$

$$\boldsymbol{S} = \sigma - \sigma_m \tag{8}$$

Where:

$\sigma_{11}, \sigma_{22}, \sigma_{33}$ …The principal stresses in three directions.

The Mises yield criterion is employed in this study to determine when material yielding occurs. The Mises stress expression is:

$$\sigma_{mises} = \sqrt{\frac{3}{2}\boldsymbol{SS}} = \sqrt{3J_2} \tag{9}$$

Where:

J_2 …The second invariant of stress, calculated from the deviatoric stress tensor.

$$J_2 = \frac{1}{2}(S_{11}^2 + S_{22}^2 + S_{33}^2 + S_{12}^2 + S_{23}^2 + S_{13}^2) \tag{10}$$

The von Mises yield function f can be written as:

$$f = \sigma_{mises} - \sigma_y = \sqrt{\frac{3}{2}\boldsymbol{SS}} - \sigma_y = 0 \tag{11}$$

Where:

σ_y …The current yield stress of the material.

When $f < 0$, the material unit is in the elastic deformation stage; when $f > 0$, the material stress exceeds the yield limit, and the material enters the viscoplastic deformation stage.

In the plastic deformation stage, the strain rate under vibration-assisted compression $\dot{\varepsilon}^p$ can be represented by the equivalent compressive plastic strain rate $\dot{\bar{\varepsilon}}^p$.

The equivalent viscoplastic strain rate $\dot{\bar{\varepsilon}}^p$. can be defined as a function of the viscoplastic strain rate $\dot{\varepsilon}^p$ [21]:

$$\dot{\bar{\varepsilon}}^p = \sqrt{\frac{2}{3}\dot{\varepsilon}^p \dot{\varepsilon}^p} \tag{12}$$

Integrating the equivalent viscoplastic strain rate $\dot{\bar{\varepsilon}}^p$. over time t yields the equivalent viscoplastic strain $\bar{\varepsilon}^p$:

$$\bar{\varepsilon}^p = \int_0^t \dot{\bar{\varepsilon}}^p d\tau \tag{13}$$

The hardening rule in viscoplastic deformation can be defined as:

$$\Delta\sigma_y = h\Delta\bar{\varepsilon}^p \tag{14}$$

The yield equation defines the yield surface $f = 0$ and elastic deformation region $f < 0$. Assuming the material satisfies the flow rule, the viscoplastic deformation rate can be expressed as:

$$\dot{\varepsilon}^p = \frac{2}{3}\frac{S}{\sigma_y}\dot{\bar{\varepsilon}}^p \tag{15}$$

This flow rule determines the increment direction of viscoplastic strain.

Eqs. (12) to (15) govern the viscoplastic evolution behavior of the material. However, these equations cannot be directly programmed and need to be converted into an incremental form through time integration. The integration procedure is as follows: first, perform an elastic prediction, i.e., calculate the equivalent stress based on purely elastic behavior using the following formula:

$$\bar{\sigma}^{pr} = \sqrt{\frac{3}{2}S^{pr}S^{pr}} \tag{16}$$

$$S_{ij}^{pr} = S_{ij}^{o} + 2\mu\Delta e_{ij} \tag{17}$$

Where the superscript o represents the result from the previous step, and pr denotes prediction.

If the elastic predicted stress $\bar{\sigma}^{pr}$ exceeds the yield stress σ_y, viscoplastic flow of the material occurs. Using the backward Euler method to integrate Eq. (15), we get:

$$\Delta\varepsilon^p = \frac{3}{2}\frac{S^{pr}}{\bar{\sigma}^{pr}}\Delta\bar{\varepsilon}^p \tag{18}$$

From Eq. (18), the expression for the equivalent viscoplastic strain increment can be derived as:

$$\Delta\bar{\varepsilon}^p = \frac{\bar{\sigma}^{pr} - \sigma_y}{3\mu + h} \tag{19}$$

The specific stress update flow chart is shown in Fig. 2.

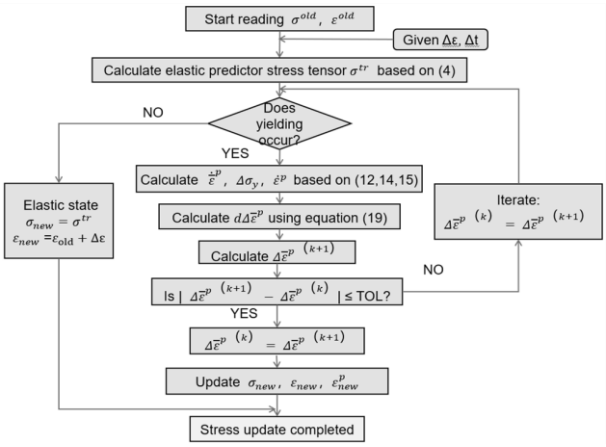

Fig. 2 *Flow Chart of Parameter Updates Based on Radial Return Algorithm*

4 Constitutive Model Subroutine Verification

In this work, the constitutive model subroutine for vibration-assisted cold upsetting forming of Ti-45Nb titanium alloy was developed using the FORTRAN programming language. The established constitutive model was linked to ABAQUS via the VUMAT user-defined subroutine interface. In the VUMAT subroutine, most material properties need to be defined by the user within the program, and the defined property values are stored in the PROPS array of the subroutine. As shown in Table 1, a total of 25 PROPS variables were defined in the program developed for this study.

Tab. 1 *Definable Material Parameters in the VUMAT Subroutine*

PROPS	1	2	3	4-7	8-16	17-25
Material Parameters	Elastic Modulus E	Poisson Ratio v	Shear Modulus G	Material Parameters	Dislocation Density Parameters	Constitutive Model Parameters

In the subroutine, the PROPS material parameters correspond to the material property values defined in the ABAQUS preprocessor. This ensures that the ABAQUS main program can access the material parameters in the constitutive model for vibration-assisted cold upsetting forming of Ti-45Nb titanium alloy at any time. Based on the relevant mechanical relationships defined in the constitutive model, ABAQUS can calculate the initial strain values and time increments, and subsequently update the stress and other related variables.

Within a single increment step of the VUMAT subroutine, the calculation of the constitutive model for Ti-45Nb titanium alloy under vibration-assisted cold upsetting forming can be divided into the following steps:

- 1) Add the keyword USER MATERIAL in the ABAQUS main program to pass the 25 material constants defined in the main program to the subroutine.
- 2) Read the stress increment and strain increment from the main program, and calculate the elastic trial stress based on the generalized Hooke's law.
- 3) Calculate the hydrostatic stress and deviatoric stress tensor from the trial stress, and then compute the von Mises equivalent stress.
- 4) Calculate the yield stress from the constitutive equations, and determine whether the material yields based on the yield function. If yielding does not occur, update the stress and state variables and proceed to the next increment.
- 5) If yielding occurs, the material enters the plastic stage. Compute the viscoplastic flow to update the equivalent plastic strain, and update the total stress and other state variables.
- 6) Update internal variables and state variables.
- 7) Complete the calculation and return control to the main program.

The computational procedure of the subroutine is illustrated in Fig. 3.

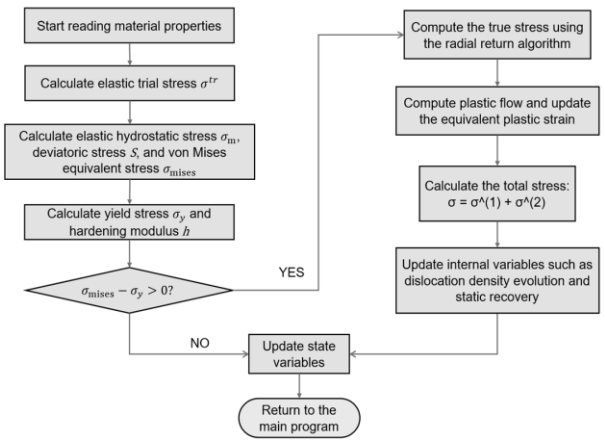

Fig. 3 *Flowchart of the VUMAT Subroutine*

The experimental verification in this study refers to the experiments reported in [22]. The experiments were conducted on Ti-45Nb titanium alloy using a servo press for low-frequency vibration-assisted upsetting tests. The specimens were annealed at 850°C and then machined into cylinders with a diameter of 3.92 mm and a height of 5 mm. Before the test, a preload of 100 N was applied to the specimen surface to prevent slipping. During the experiment, the upper punch was pressed downward at a rate of 0.1 mm/s while superimposing low-frequency sinusoidal vibration. The load data were collected in real time by a pressure sensor mounted on the tool head, with a sampling frequency of 30 Hz and a resolution of 50 N. The punch, die, and specimen were modeled according to the experimental setup, with the specific model information shown in Table 2. Since the deformation of the die and punch is negligible compared with the specimen in the actual experiment, they were treated as rigid bodies in the simulation. The three-dimensional finite element model is shown in Fig. 4. To match the experimental conditions, the die was fully constrained, and the punch was applied with downward vibration-assisted displacement. The friction coefficient between the specimen and the punch/die was set to 0.8. The punch feed rate was 0.1 mm/s, and a total strain of 50% was applied.

Tab. 2 *Finite element model information*

Model	Diameter (mm)	Height (mm)	Element Type	Number of Elements	Material
Specimen	3.92	5	C3D8	20895	Ti-45Nb
Die	10	3	C3D8	232	Rigid body
Punch	6	15	C3D8	610	Rigid body

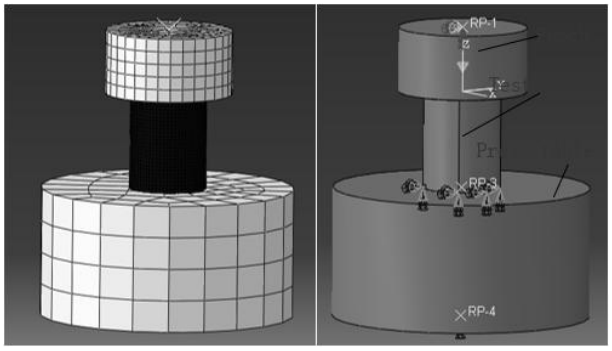

Fig. 4 *Experimental 3D finite element model*

The VUMAT subroutine was used to simulate the 3D model of Ti-45Nb titanium alloy vibration-assisted cold upsetting forming. Seven sets of vibration parameters were simulated (Where A represents the vibration amplitude, and F represents the vibration frequency): no vibration, A=0,05mm, F=10Hz; A=0,1mm, F=10Hz; A=0,2mm, F=10Hz; A=0,3mm, F=10Hz; A=0,1mm, F=20Hz; and A=0,1mm, F=30Hz. The stress-strain curves obtained from the simulation were compared with experimental results, as shown in Fig. 5.

From the comparison of different conditions in Fig 5, it can be seen that the VUMAT subroutine simulation results have a slightly better fit with the experimental data in the viscoplastic stage than in the elastic stage. This is mainly because the viscoplastic forming stage involves larger deformations and more fitting parameters, which have a greater impact on forming flow. Therefore, when fitting parameters, the focus was on the plastic forming stage. However, overall, the fitting results are very close.

To quantify the simulation accuracy of the VUMAT subroutine, the average relative error of the simulation data was calculated, as shown in Table 3.

Tab. 3 *Average Relative Error of Simulation Results*

Amplitude/mm	Frequency/Hz	VUMAT Subroutine Error (%)
0	0	4.38
0.1	10	3.23
0.1	20	3.69
0.1	30	2.72
0.05	10	4.67
0.1	10	3.23
0.2	10	3.71
0.3	10	4.49

As shown in Table 3, the average relative error between the simulation results of the VUMAT subroutine and the experimental data is less than 5%, quantitatively demonstrating that the secondary-developed Ti-45Nb titanium alloy vibration - assisted cold upsetting forming constitutive model subroutine in this paper has high precision and good consistency with the actual material properties.

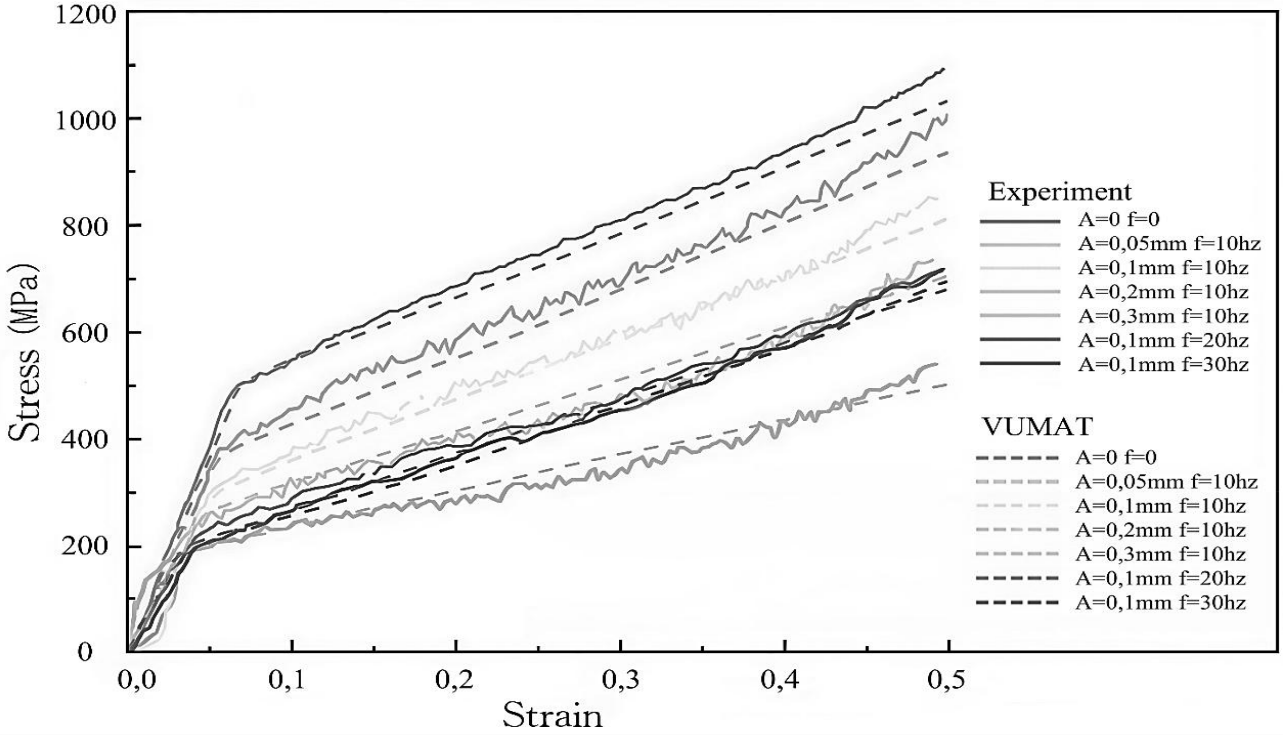

Fig. 5 *Comparison of VUMAT Subroutine Simulation Results and Experimental Data*

5 Application of the Constitutive Model

Taking the Ti-45Nb internal wire joint as the application object, the internal wire joint connector is a cylindrical tubular part. Cold upsetting forming in a single operation is challenging. To ensure part forming quality, the cold upsetting process for the internal wire joint is divided into five steps: (1) reshaping; (2) necking; (3) compound extrusion; (4) boss forming; (5) drilling and trimming, as shown in Figure 6. This study primarily focuses on simulation research of the first four steps in multi-pass cold upsetting forming.

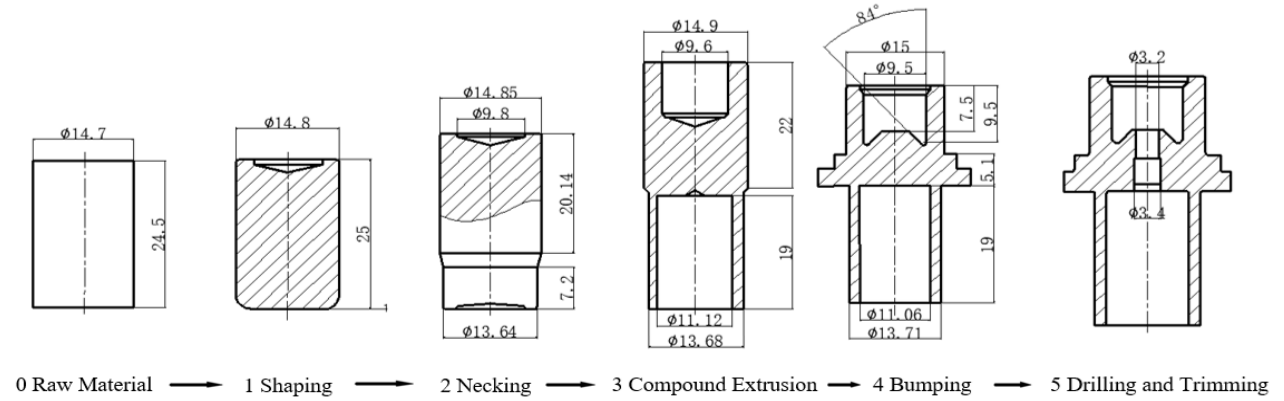

Fig. 6 *Inner wire joint parts forming process diagram (mm)*

5.1 Finite Element Model Establishment

Based on the drawings of the internal-thread connector, the component and the corresponding cold forging dies were modeled using SolidWorks. Since the component has an axisymmetric geometry, a 1/4 model was selected for the simulation.

Since cold forging is employed, the forging environment temperature was set to room temperature (20°C). The workpiece material is Ti-45Nb titanium alloy, and the previously developed constitutive model for vibration-assisted cold forging of Ti-45Nb was used in the simulation. The mesh was generated with a minimum element edge length

of 0.3 mm, resulting in a total of 58,168 elements for the workpiece. The cold forging die files were imported, with the die material selected as AISI H-13 and modeled as a rigid material. The material parameters of the die are listed in Table 4, and the die mesh contains 1,384 elements.

Tab. 4 *Mold material parameters [23]*

Mold Material	Density (kg/m³)	Elastic Modulus (GPa)	Poisson's Ratio	Thermal Expansion Coefficient (1/K)	Specific Heat (J/kg·K)	Thermal Conductivity (W/m·K)
AISI H-13	7.76×10^3	193	0.26	1.18×10^{-5}	460	28.5

In actual forming processes, the billet comes into contact with the mold and generates friction. Therefore, it is necessary to set an appropriate friction coefficient to reflect the actual conditions. In the finite element simulation, the contact between the billet and the upper/lower molds is defined, with finite sliding selected for the surface sliding behavior, and the friction coefficient is set to 0.08.

During vibration-assisted cold upsetting forming, the vibration effect is typically achieved by applying axial or transverse vibrations to the mold. In this study, axial vibration is applied to the punch during its feed motion. Consequently, the actual motion speed of the punch is obtained by superimposing the linear feed speed and the axial vibration speed. The feed speed of the punch is set to 39 mm/s, and the applied vibration parameters are an amplitude of 20 μm and a frequency of 400 Hz. The reason for selecting 400 Hz is twofold: on the one hand, this frequency falls within the typical range of mechanical vibrations, making it easier to achieve stable output in engineering equipment while avoiding certain structural resonance frequencies [24]; on the other hand, the constitutive model established in this paper is based on the viscoelastic-plastic theoretical framework, where the vibration effects are characterized by the material viscosity coefficients (η_1, η_2) and the vibration energy field parameters (θ, n). The physical mechanism of this model remains consistent over a wide frequency range (from tens to hundreds of Hertz). The VUMAT subroutine file is imported for calculation. The forming results of each step are shown in Figure 7. The results indicate that the material filling is complete in all four steps, without folding, damage, or other defects.

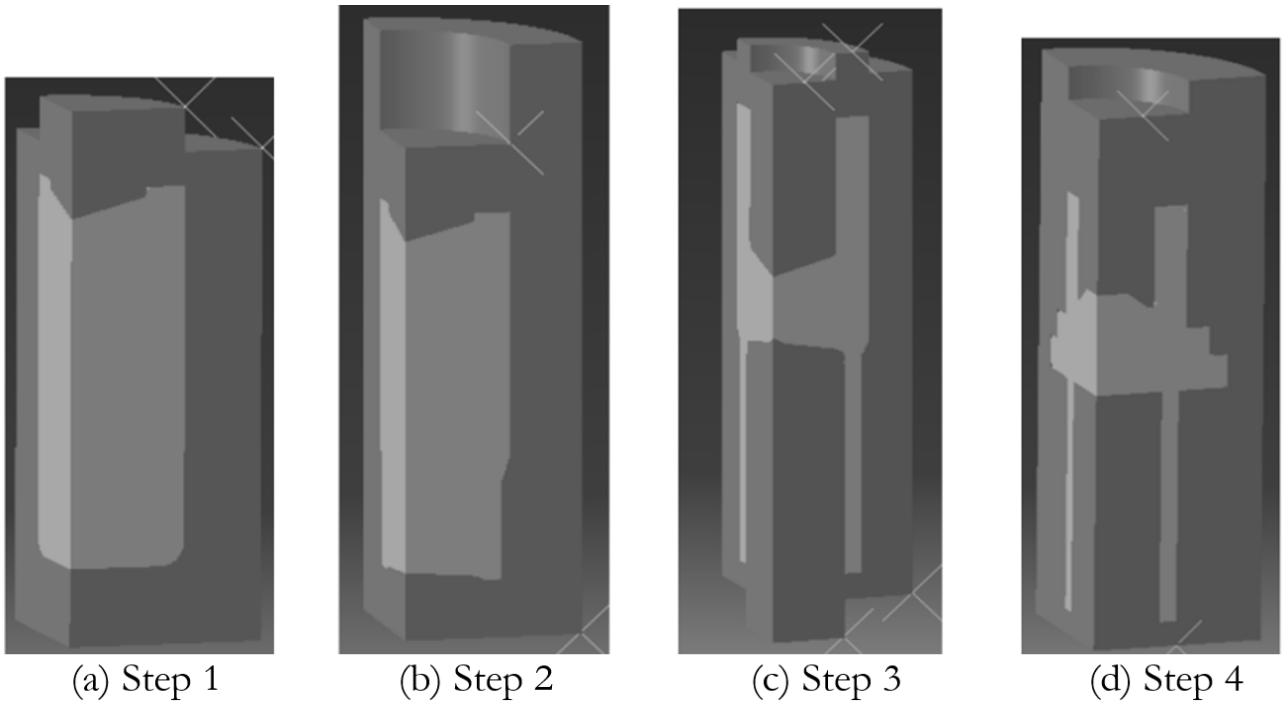

Fig. 7 *Forming Results of Each Step*

5.2 Simulation Result Analysis

5.2.1 Equivalent Stress Analysis

Equivalent stress is a concept used to describe the stress state of materials, simplifying the complex stress state into a single scalar value. It clearly reflects the stress distribution across the model, helps identify high-stress regions, recognizes potential defect locations, and reveals potential issues in the process

design. Figure 8 presents the stress distribution cloud charts for each step of conventional cold upsetting forming and vibration-assisted cold upsetting forming. The vibration-assisted parameters are set to an amplitude of 20 μm and a frequency of 400 Hz.

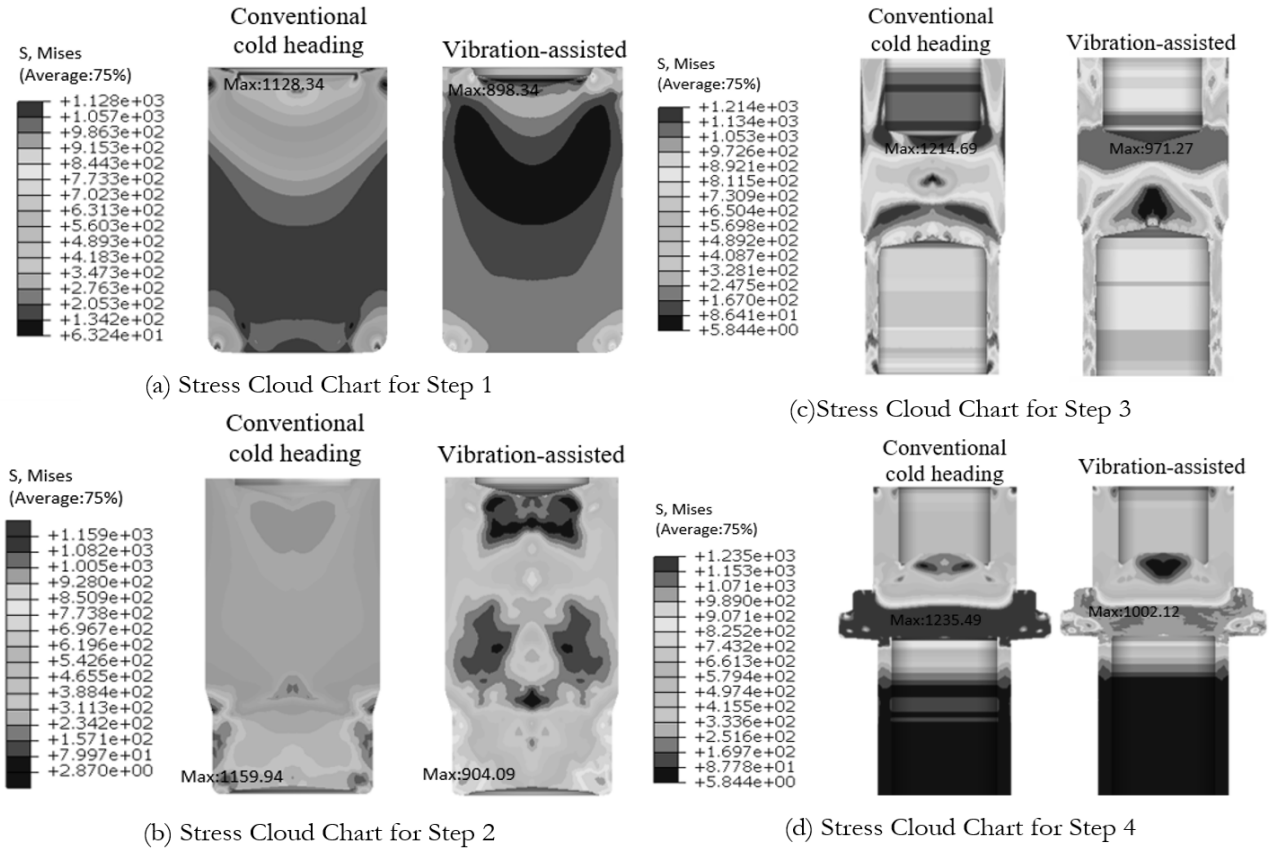

(a) Stress Cloud Chart for Step 1

(c)Stress Cloud Chart for Step 3

(b) Stress Cloud Chart for Step 2

(d) Stress Cloud Chart for Step 4

Fig. 8 *Stress Distribution Diagram of Each Cold Upsetting Forming Step*

Comparing the stress distribution cloud charts of conventional cold upsetting forming and vibration-assisted cold upsetting forming, it is evident that the position of maximum stress remains unchanged after vibration assistance, but the stress distribution becomes more uniform, with a significant reduction in maximum stress values. With vibration-assisted cold upsetting forming, the maximum stress in Step 1 decreases by approximately 20.4%; in Step 2, by approximately 22.1%; in Step 3, by approximately 20.1%; and in Step 4, by approximately 18.9%. Additionally, the size of high-stress regions in each step is markedly reduced.

5.2.2 Equivalent Strain Analysis

Equivalent strain is a concept used to describe material deformation, simplifying the multi-axial strain state under complex loading conditions into a single scalar value. It clearly reflects the deformation distribution across the model, helps identify regions with significant deformation, recognizes potential sites for damage or failure, and reveals potential issues in the forming process. From the strain cloud chart variations in Figure 9, it can be observed that during Step 3 (compound extrusion), the maximum equivalent strain occurs on the inner side of the thin wall. However, in this stage, the introduction of vibration assistance promotes material flow on the inner side of the thin wall, significantly reducing the strain in this region.

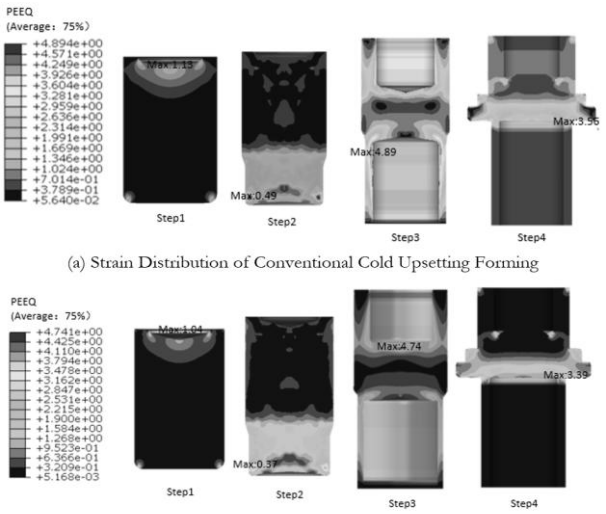

(a) Strain Distribution of Conventional Cold Upsetting Forming

(b) Strain Distribution of Vibration-Assisted Cold Upsetting Forming

Fig. 9 *Strain Distribution Diagram of Each Cold Upsetting Forming Step*

By comparing the workpiece internal strain distribution charts in Figure 9 (a) and (b), it is evident that vibration improves material flow, reduces internal workpiece strain, and makes its distribution more uniform.

This chapter combines the Ti-45Nb titanium alloy internal wire joint parts from enterprise production with vibration-assisted cold upsetting forming technology and employs the self-developed VUMAT subroutine constitutive model for simulation. Through finite element simulation, the impact of vibration assistance on stress and strain during forming is intuitively observed, revealing its significant effects in reducing maximum stress, optimizing stress distribution, and improving material flow. The VUMAT subroutine constitutive model, combined with finite element simulation technology, accurately simulates the stress and strain distribution in vibration-assisted cold upsetting forming, providing a scientific basis for optimizing process parameters and die design.

6 Conclusions

This paper establishes a visco-elastoplastic constitutive model for Ti-45Nb titanium alloy vibration-assisted cold upsetting forming. The model is algorithmically transformed by deriving its incremental form using the backward Euler method and is implemented in simulations through the VUMAT interface of ABAQUS. Experimental comparisons show that the model aligns well with experimental data in the viscoplastic stage, with an overall average relative error of less than 5%, thus verifying its reliability. This provides an efficient tool for the numerical simulation of Ti-45Nb titanium alloy vibration-assisted cold upsetting forming. The VUMAT subroutine constitutive model developed in this paper is used to simulate the cold upsetting forming process of internal thread joints made of Ti-45Nb titanium alloy. It can intuitively observe the influence of vibration assistance on stress and strain during the forming process. It is found that vibration assistance can enhance the plastic deformation capacity of Ti-45Nb titanium alloy in the cold upsetting forming process and make the stress distribution more uniform. In future work, experimental verification under higher frequency conditions will be carried out to further expand the applicable boundary of the proposed model.

Acknowledgement

The Project is supported by Ningbo "Science and technology innovation Yongjiang 2035" key research and development program (2024Z169).

References

[1] LU, W. H. (2023). Research and improvement of multi-station cold forging process for automotive flange connecting parts based on numerical simulation. *Forging & Stamping Technology,* Vol. 48, No. 2, pp. 29-35+110. DOI: 10.13330/j.issn.1000-3940.2023.02.004.

[2] CHENG, M. W., LIU, F. L., LI, W. Q., et al. (2020). Research on the microstructure evolution law of multi-station heading forming of stainless steel high lock nuts. *Hot Working Technology*, Vol. 49, No. 5, pp. 103-107. DOI: 10.14158/j.cnki.1001-3814.20183526.

[3] YU, F. Q., FANG, Z. L. (2023). Research on ultrasonic vibration-assisted milling process for titanium alloy thin-walled parts. *Mechanical and Electrical Engineering,* Vol. 40, No. 1, pp. 129-135.

[4] LI, Y. B., LIU, T. D. (2022). Research on the microstructure and properties of cast TC4 titanium alloy. *Hot Working Technology*, Vol. 51, No. 21, pp. 65-68. DOI: 10.14158/j.cnki.1001-3814.20211439

[5] QI, Z. C., XIAO, Y. X., WANG, X. X., et al. (2021). Analysis of the forming performance of Ti45Nb rivets under pulse current-assisted pressing. *China Mechanical Engineering,* Vol. 32, No. 23, pp. 2832-2839, 2849.

[6] TENG, X. Y. (2021). Simulation research on the flexible coupling model of the transmission mechanism of high-speed cold heading machine. Jinan University.

[7] YANG, L. J., CHEN, X., SUN, B. S. (2023). Simulation analysis of the forming law of TC4 titanium alloy tube under vibration-assisted forming. *Hot Working Technology*, Vol. 52, No. 5, pp. 102-107. DOI: 10.14158/j.cnki.1001-3814.20210219

[8] HU, J., SHIMIZU, T., YOSHINO, T., et al. (2018). Ultrasonic dynamic impact effect on deformation of aluminum during micro-compression tests. *Journal of Materials Processing Technology*, Vol. 258, pp. 144-154. DOI: 10.1016/j.jmatprotec.2018.03.021

[9] ZHANG, H. D., DENG, L., WANG, X. Y., et al. (2020). Research progress on the mechanism and application of vibration-assisted plastic forming. *Aeronautical Manufacturing Technology*, Vol. 63, No. 16, pp. 22-31. DOI: 10.16080/j.issn1671-833x.2020.16.022

[10] GUO, L. G., WANG, F. Q., LIANG, L., et al. (2017). New ideas and research progress on

intelligent simulation optimization of high-performance ring rolling forming. *Precision Forming Engineering,* Vol. 9, No. 4, pp. 1-11. DOI: 10.3969/j.issn.1674-6457.2017.04.001

[11] WANG, Z. J., WANG, Z. W. (2024). Simulation research on metal tensile testing based on J-C constitutive model. *Xinjiang Steel,* No. 2, pp. 31-33.

[12] WANG, Z., YIN, H. (2025). Titanium Alloy Turning Machining Model and Quality Analysis Based on Finite Element Analysis. *Manufacturing Technology*, Vol. 25, No. 3, pp. 413-423. DOI: 10.21062/mft.2025.036.

[13] KIRCHNER, H. O. K., KROMP, W., PRINZ, F. B., et al. (1985). Plastic deformation under simultaneous cyclic and unidirectional loading at low and ultrasonic frequencies. *Materials Science and Engineering,* Vol. 68, No. 2, pp. 197-206. DOI：10.1016/0025-5416(85)90409-4

[14] CAI, G. P., LIU, Z., ZHAN, H. (2008). Volume effect analysis of metal deformation with low-frequency pulse vibration. *Forging & Stamping Technology,* No. 5, pp. 155-159.

[15] WANG, J. P., ZHAO, Z., ZHUANG, X. C., et al. (2015). Study on constitutive model of ultrasonic vibration-assisted forming. *Journal of Plasticity Engineering,* Vol. 22, No. 6, pp. 1-6. DOI: 10.3969/j.issn.1007-2012.2015.06.001

[16] SIDDIQ, A., SAYED, T. E. (2011). Acoustic softening in metals during ultrasonic assisted deformation via CP-FEM. *Materials Letters*, Vol. 65, No. 2, pp. 356-359.DOI: 10.1016/j.matlet.2010.10.029

[17] MELLER, A., LEGUTKO, S., MRÓZ, A., et al. (2024). Enhancing Durability of Multi-Cavity Forging Tools through Process Automation. *Manufacturing Technology*, Vol. 24, No. 6, pp. 929-939. DOI: 10.21062/mft.2024.105.

[18] LIU, Z. J. (2024). Research on titanium alloy milling simulation platform and cutting characteristics based on Abaqus. Shenyang Ligong University. DOI: 10.27323/d.cnki.gsgyc.2024.000672.

[19] Zeng X. G., Chen H. Q., Chen J., (2016) Viscoelastic Mechanics. Chengdu: Sichuan University Press.

[20] Yao Z., Kim G. Y., Wang Z., et al. (2012) Acoustic softening and residual hardening in aluminum: modeling and experiments[J]. *International Journal of Plasticity,* 2012, 39: 75-87. DOI: 10.1016/j.ijplas.2012.06.003

[21] NAGODE M., KLEMENC J., OMAN S., et al. (2024) Elasto-viscoplastic material modelling using the multiaxial Prandtl operator approach. *International Journal of Mechanical Sciences*, Vol. 267, pp. 108953. DOI: 10.1016/j.ijmecsci.2023.108953

[22] LIN, J., PRUNCU, C., ZHU, L., et al. (2022). Deformation behavior and microstructure in the low-frequency vibration upsetting of titanium alloy. *Journal of Materials Processing Technology*, Vol. 299, p. 117360. DOI: 10.1016/j.jmatprotec.2021.117360.

[23] SHI, Y. P., ZHOU, Y. R. (2006). *ABAQUS Finite Element Analysis Example Explanation*. Beijing: Mechanical Industry Press.

[24] ZHENG, B. (2024). Analysis of Static and Dynamic Characteristics and Lightweight Design of Titanium Alloy Frame. *Manufacturing Technology*, Vol. 24, No. 3, pp. 507-519. DOI: 10.21062/mft.2024.053.